ACS OMEGA

http://pubs.acs.org/journal/acsodf

Article

Protonation-Induced Hyperporphyrin Spectra of *meso*-Aminophenylcorroles

Ivar K. Thomassen and Abhik Ghosh*

Cite This: *ACS Omega* 2020, 5, 9023−9030

Read Online

ACCESS | Metrics & More | Article Recommendations

ABSTRACT: UV−vis spectrophotometric titrations have been carried out on *meso*-tris(*o*/*m*/*p*-aminophenyl)corrole (H_3[*o*/*m*/*p*-TAPC]) and *meso*-triphenylcorrole (H_3[TPC]) in dimethyl sulfoxide with methanesulfonic acid (MSA). Monoprotonation was found to result in hyperporphyrin spectra characterized by new, red-shifted, and intense Q bands. The effect was particularly dramatic for H_3[*p*-TAPC] for which the Q band red-shifted from ∼637 nm for the neutral species to 764 nm in the near-IR for H_4[*p*-TAPC]$^+$. Upon further protonation, the Q band was found to blue-shift back to 687 nm. A simple explanation of the phenomena has been offered in terms of quinonoid resonance forms.

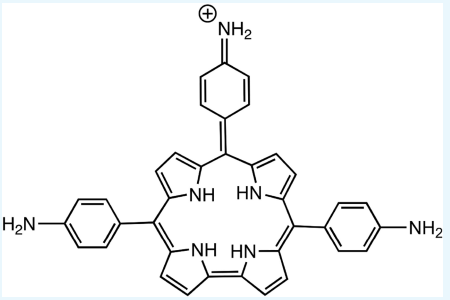

1. INTRODUCTION

The electronic spectra of porphyrins were classified by Gouterman and co-workers as normal, hypso, and hyper.[1,2] Normal spectra are observed for free-base and many non-transition element derivatives of simple porphyrins such as tetraphenyl- or octaethylporphyrin and are characterized by the classic Soret and Q bands as well as by an N band in the near-UV. Hypsoporphyrins exhibit blue-shifted Soret and Q bands, while hyperporphyrins exhibit extra bands relative to normal porphyrins at wavelengths above 300 nm. Unlike normal spectra, which are dominated by porphyrin $\pi \rightarrow \pi^*$ transitions, hyper spectra also involve additional types of transitions, notably charge transfer (CT) transitions. Heme-thiolate proteins and their model compounds provide many examples of hyperporphyrins.[3,4] Diprotonated tetraarylporphyrins provide another important class of hyperporphyrins; the spectra of these species exhibit additional bands attributed to aryl-to-porphyrin CT transitions. Protonated *meso*-aminophenylporphyrins provide particularly vivid examples of such spectra.[5−12] An entirely analogous effect is also observed for *meso*-tetrakis(*p*-hydroxyphenyl)porphyrin in alkaline media where the spectra exhibit extra bands due to phenolate-to-porphyrin CT transitions.[13,14]

Hyper spectra are also well-established for metallocorroles. Indeed, many metallotriarylcorroles formally described as M^{n+}−corrole^{3-} are actually better described as $M^{(n-1)+}$−corrole$^{\cdot 2-}$ and exhibit substituent-sensitive Soret bands with substantial aryl-to-corrole$^{\cdot 2-}$ charge-transfer character.[15−18] Examples of such noninnocent metallocorroles include MnCl,[19] FeCl,[20−23] FeNO,[23−25] Co,[26−28] and Cu[29−34] corroles. Although the Soret bands of innocent metallotriarylcorroles do not exhibit the same kind of substituent sensitivity as their noninnocent counterparts, many exhibit overall hyper-type spectra, reflecting corrole(π)-to-metal(d) transitions. Many families of 5d metallocorroles recently reported from our laboratory exhibit such spectra. Thus, $Re^{V}O$,[35] $Os^{VI}N$,[36] Pt,[37,38] and Au[39−41] corroles all exhibit redshifted Soret bands and sharp, split Q bands. Little, however, has been documented vis-à-vis the potential hyper character of protonated free-base triarylcorroles,[42,43] in particular *meso*-aminophenylcorroles. Herein, we show that these systems, upon protonation, exhibit dramatically redshifted Q bands and thus spectra that are aptly described as hyper.

2. RESULTS

Spectrophotometric titrations were carried out on approximately 0.03 mM solutions of tris(o^{44}/m^{45}/p^{46}-aminophenyl)corrole (H_3[*o*/*m*/*p*-TAPC]) and triphenylcorrole (H_3[TPC])[31] (Chart 1) in dimethyl sulfoxide (DMSO) with methanesulfonic acid (MSA) in DMSO (with concentrations ranging from about 1 mM to pure MSA) as titrant (Figures 1−4). Even sub-equivalent amounts of MSA led to substantial spectral changes, consistent with neutralization of the anionic $CorH_2^-$ state that is thought to be present in substantial amounts in DMSO solutions.[47] Interestingly, although we could identify peaks that are reasonably attributable to the anions, the broad peaks that were generated in the Q region could not be definitively assigned to a single species such as the neutral corrole (Table 1).

Received: March 9, 2020
Accepted: March 24, 2020
Published: April 6, 2020

https://dx.doi.org/10.1021/acsomega.0c01068
ACS Omega 2020, 5, 9023−9030

Chart 1. Compounds Studied in this Work

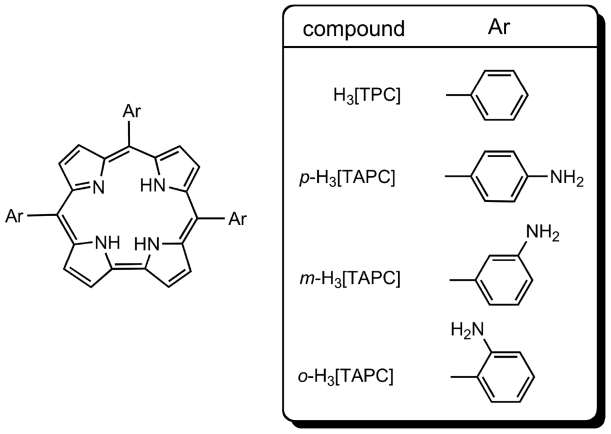

On the whole, it was clear that neutralization of the anionic states results in a weakening of both the Soret and Q bands.

Further addition of MSA resulted in dramatic redshifts and intensification of the Q bands. For H_3[*p*-TAPC] (Figure 1), the Q band shifted from the mid-600s to ~764 nm, i.e., into the near-infrared, with the addition of a few equivalents of MSA. For H_3[*o*-TAPC] (Figure 3), the Q bands at 575 and 610 nm disappeared and a strong Q band grew at 676 nm, albeit with the addition of larger quantities of MSA (a couple of hundred equivalents). Qualitatively similar changes were also observed for H_3[TPC] (Figure 4), with disappearance of the Q bands at 585 and 618 nm and appearance of a strong Q band at 685 nm. The final spectra were strongly suggestive of hyper character, attributable at least in part to phenyl-to-corrole charge transfer in the H_4[*p*-TAPC]$^+$ and H_4[TPC]$^+$ cations. The formation of these monocations was also accompanied by a slight weakening of the Soret band.

Addition of a large excess (i.e., thousands of equivalents) of MSA to H_3[*o*/*m*/*p*-TAPC] solutions led to further changes, consistent with the formation of H_5[*o*/*m*/*p*-TAPC]$^{2+}$ dications. The spectral changes are arguably most dramatic for H_3[*p*-TAPC] (Figure 1) where the Q band blueshifts dramatically from 764 to 687 nm, while a new blue-shifted Soret feature grows at 430 nm. Understandably, H_3[TPC] (Figure 4), which lacks peripheral amino groups, did not evince any indication of dication formation under the experimental conditions. We also could not discern whether tri- and tetracationic states of H_3[*o*/*m*/*p*-TAPC] formed under the conditions of the experiments.

The dramatic spectral changes associated with the formation of $CorH_4^+$ species allowed us to qualitatively estimate the relative basicities of the four corroles in terms of the apparent $pK_{a\text{-}app}$'s of the $CorH_4^+$ species. In this approach, used earlier by Wamser and co-workers for aminophenylporphyrins,[9] $pK_{a\text{-}app}$ simply equals the negative logarithm of the analytical concentration of MSA at the half-equivalence point, which was estimated from spectral changes at multiple wavelengths. Using this approach, we estimated $pK_{a\text{-}app}$ values of 5.2 ± 0.1 for

Table 1. UV−vis Absorption Maxima of Different Protonation States of the Free-Base Corroles Studied

	$CorH_2^-$		$CorH_3$		$CorH_4^+$		$CorH_5^{2+}$	
compound	Soret	Q	Soret	Q	Soret	Q	Soret	Q
H_3[*p*-TAPC]	430[a]	655[a]	429[a,b]	526[a], 637[a]	454[a]	547, 622, 764[a]	430[a], 458	687[a]
H_3[*m*-TAPC]	427[a], 449	643[a]	416[a,c]	572[a], 614, 646	428[a], 460	690[a]	431[a]	684[a]
H_3[*o*-TAPC][d]	425[a]	578, 632[a]	414[a,c]	518, 566[a], 604, 638	422[a]	676[a]	424[a]	655[a]
H_3[TPC]	427[a], 448	641[a]	415[a,c]	567[a], 615, 648	427[a], 458	685[a]		

[a]The strongest peak in each set is marked with an asterisk. [b]In acetone.[45] [c]In dichloromethane.[46] [d]Mixture of atropisomers.[44]

Scheme 1. Principal Resonance Structures of the Mono- and Diprotonated Forms of H_3[*p*-TAPC]

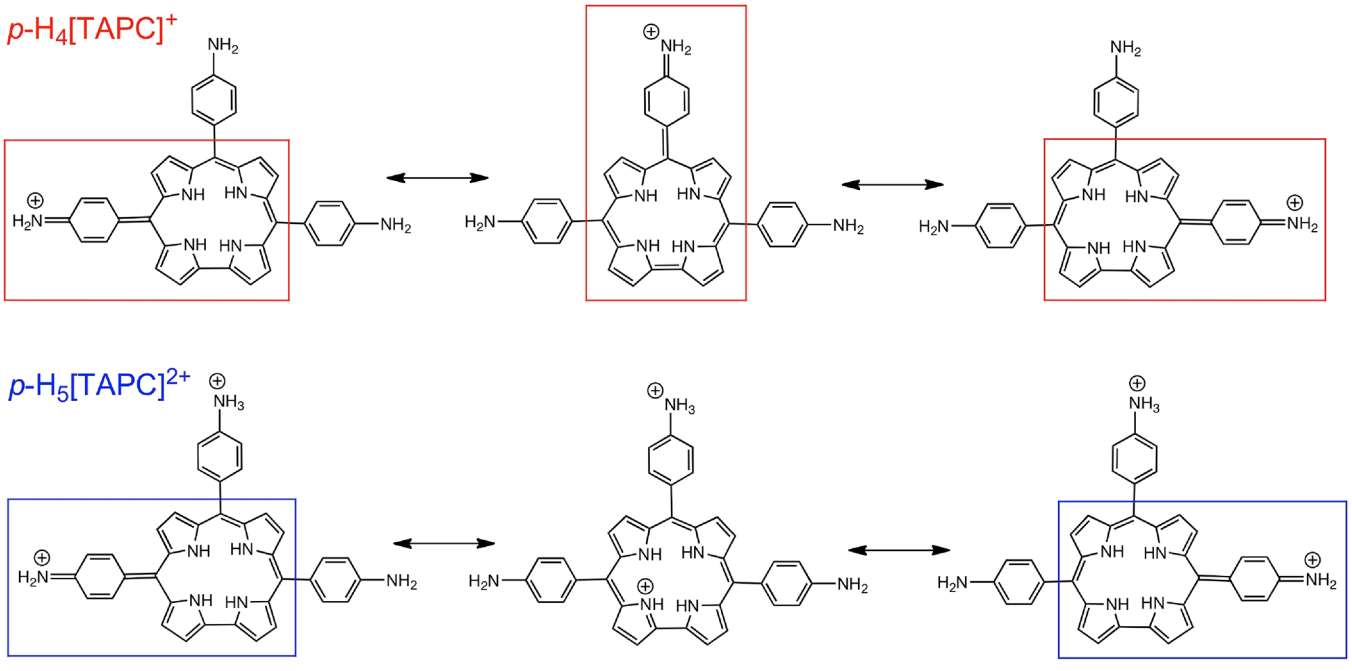

https://dx.doi.org/10.1021/acsomega.0c01068
ACS Omega 2020, 5, 9023−9030

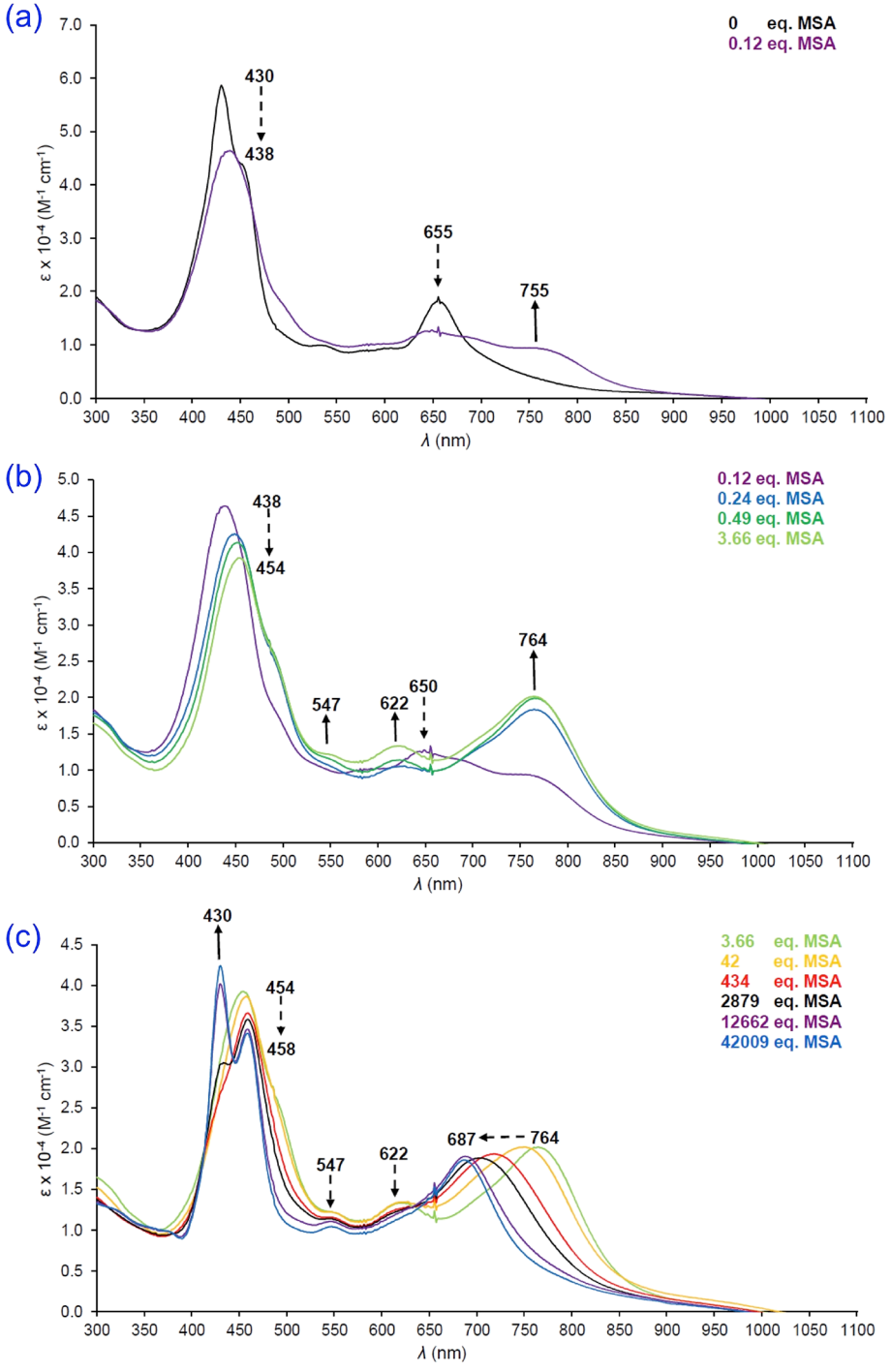

Figure 1. Spectral changes for *p*-H_3[TAPC] in DMSO as a function of added equivalents of MSA. The three panels approximately correspond to the following transformations: (a) $CorH_2^-$ → $CorH_3$, (b) $CorH_3$ → $CorH_4^+$, and (c) $CorH_4^+$ → $CorH_5^{2+}$.

both H_3[*p*-TAPC] and H_3[*m*-TAPC], 4.5 ± 0.1 for H_3[*o*-TAPC], and 4.1 ± 0.1 for H_3[TPC]. In other words, the first two compounds are somewhat more basic than the latter two compounds (by just under a factor of 10), potentially reflecting steric inhibition of resonance interactions for the ortho isomer.

3. DISCUSSION

The spectral changes accompanying the formation of $CorH_4^+$ species are reminiscent of those accompanying the formation of centrally diprotonated tetraarylporphyrins, in particular tetrakis-(*p*-aminophenyl)porphyrin (H_2[*p*-TAPP]). The redshift of the Q band accompanying the generation of H_4[*p*-TAPP]$^{2+}$, however, is larger than that accompanying the generation of H_4[*p*-TAPC]$^+$. Thus, the Q band at approx. 637 nm for H_2[*p*-TAPP] redshifts to approx. 811 nm for H_4[*p*-TAPP]$^{2+}$.[7−9] For H_3[*p*-TAPC], the Q band shifts from 669 nm for the neutral species to 764 nm for *p*-H_4[*p*-TAPC]$^+$. The lower spectral shift in the latter case may reflect the lower positive charge of H_4[*p*-TAPC]$^+$ relative to H_4[*p*-TAPP]$^{2+}$. Alternatively, or additionally, the lower spectral shift for corrole protonation may be related to the fact that a smaller geometrical change is involved; free-base corroles are already strongly nonplanar and proto-

https://dx.doi.org/10.1021/acsomega.0c01068
ACS Omega 2020, 5, 9023−9030

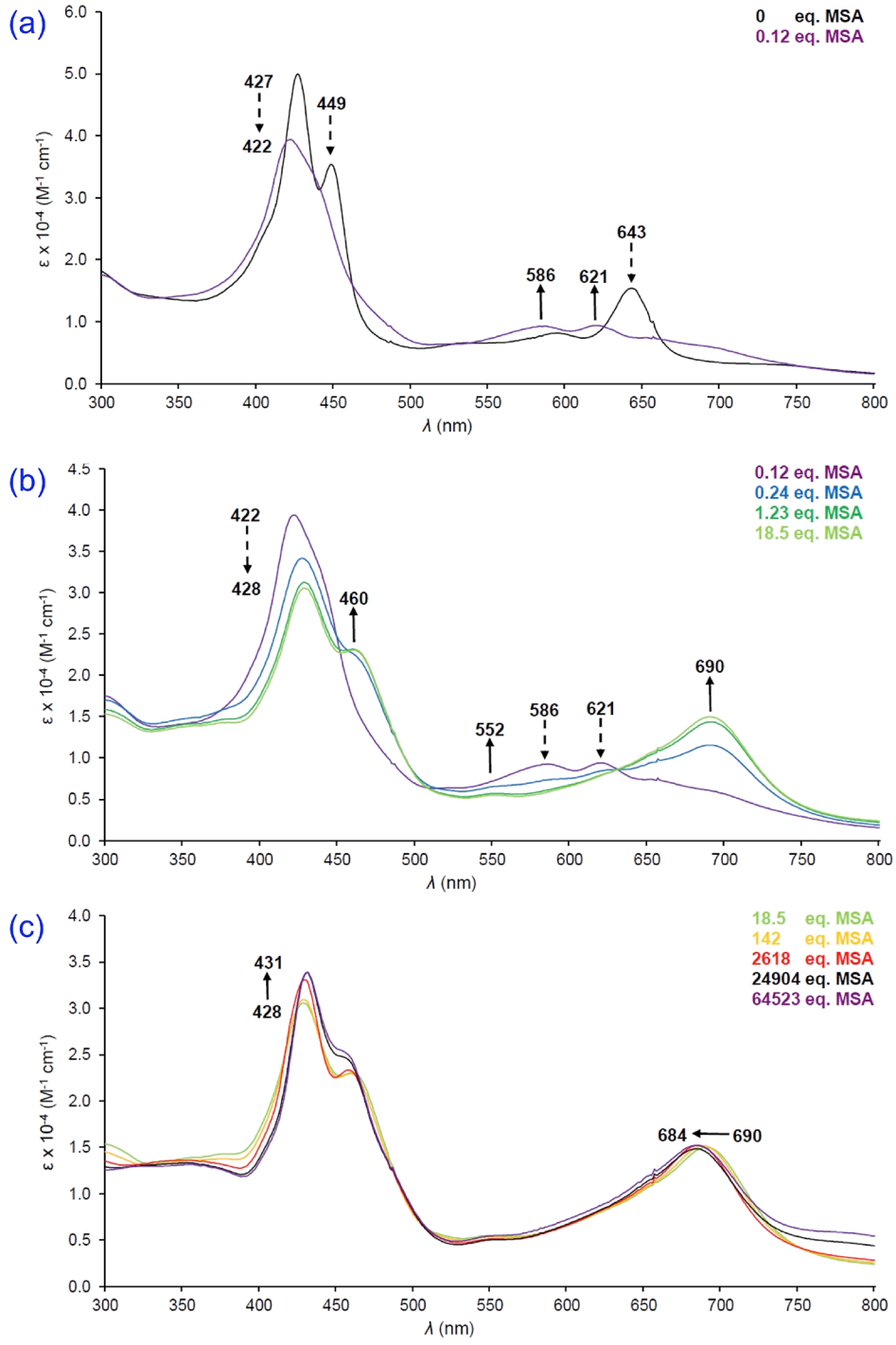

Figure 2. Spectral changes for *m*-H_3[TAPC] in DMSO as a function of added equivalents of MSA. The three panels approximately correspond to the following transformations: (a) $CorH_2^- \rightarrow CorH_3$, (b) $CorH_3 \rightarrow CorH_4^+$, and (c) $CorH_4^+ \rightarrow CorH_5^{2+}$.

nation results in only a modest increase in nonplanarity. For H_2[*p*-TAPP], in contrast, protonation of two central nitrogens alters the macrocycle conformation from planar to strongly saddled.[48−50]

It would be of great interest to simulate the above spectral shifts by quantum chemical means and thereby dissect the contributions of different factors such as charge transfer, conformation, and substituents on the *meso*-aryl groups. Such calculations, however, involve considerable challenges largely because charge transfer transitions have long been a weakness for time-dependent density functional theory methods;[51−53] a recent CAM-B3LYP and CC2 study of tetraphenylthiaporphyrin, tetraphenylporphyrin *N*-oxide, and their protonation, however, have yielded promising results and may point to a way forward.[54] Meanwhile, as discussed by Wamser and coworkers for porphyrins,[9] simple consideration of resonance forms may provide a qualitative explanation of some of the observed spectral shifts. Thus, the strongly redshifted Q band of H_4[*p*-TAPC]$^+$ seems ascribable to the three quinonoid resonance forms shown in Scheme 1, whereas the comparatively blue-shifted Q band of the H_4[*p*-TAPC]$^{2+}$ dication seems ascribable to only two quinonoid resonance forms.

https://dx.doi.org/10.1021/acsomega.0c01068
ACS Omega 2020, 5, 9023−9030

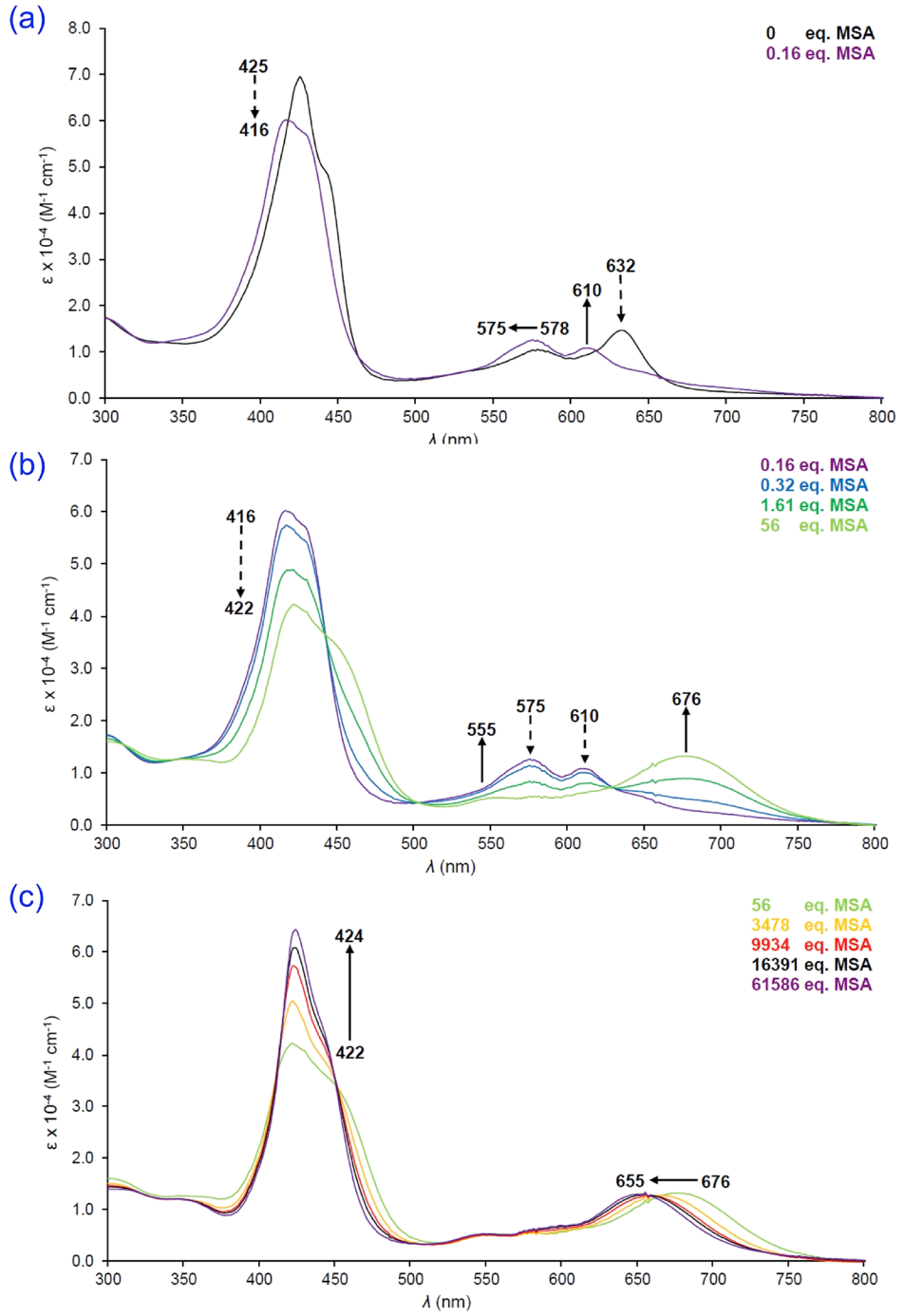

Figure 3. Spectral changes for *o*-H_3[TAPC] in DMSO as a function of added equivalents of MSA. The three panels approximately correspond to the following transformations: (a) $CorH_2^-$ → $CorH_3$, (b) $CorH_3$ → $CorH_4^+$, and (c) $CorH_4^+$ → $CorH_5^{2+}$.

4. CONCLUSIONS

UV−vis spectrophotometric titration of the *ortho*, *meta*, and *para* isomers of H_3[TAPC] and H_3[TPC] was carried out in DMSO with methanesulfonic acid (MSA). For all the compounds, monoprotonation led to hyperporphyrin spectra with strongly red-shifted and intense Q bands. The effect was especially dramatic for H_3[*p*-TAPC] for which the Q band was found to red-shift from ∼637 nm for the neutral species to 764 nm in the near-IR for H_4[*p*-TAPC]$^+$. Upon further protonation, the Q band was found to blue-shift back to 687 nm. A simple explanation of the phenomena has been formulated in terms of quinonoid resonance forms.

5. EXPERIMENTAL SECTION

The *ortho*, *meta*, and *para* isomers of H_3[TAPC] and H_3[TPC] were all freshly prepared as previously described and yielded ^{1}H NMR and mass spectroscopic data in accord with the literature.[44−46] UV−vis spectrophotometric titrations were carried out on an HP 8453 spectrophotometer using solutions of methanesulfonic acid in anhydrous DMSO. Corrole solutions were prepared from anhydrous DMSO and purged with argon prior to use. Titrations were performed in a cuvette with an initial corrole solution of 400 μL. Acid additions were performed using a micropipette in gradual increments from 2 to 20 μL, depending on the acid concentration. After each addition, the

https://dx.doi.org/10.1021/acsomega.0c01068
ACS Omega 2020, 5, 9023−9030

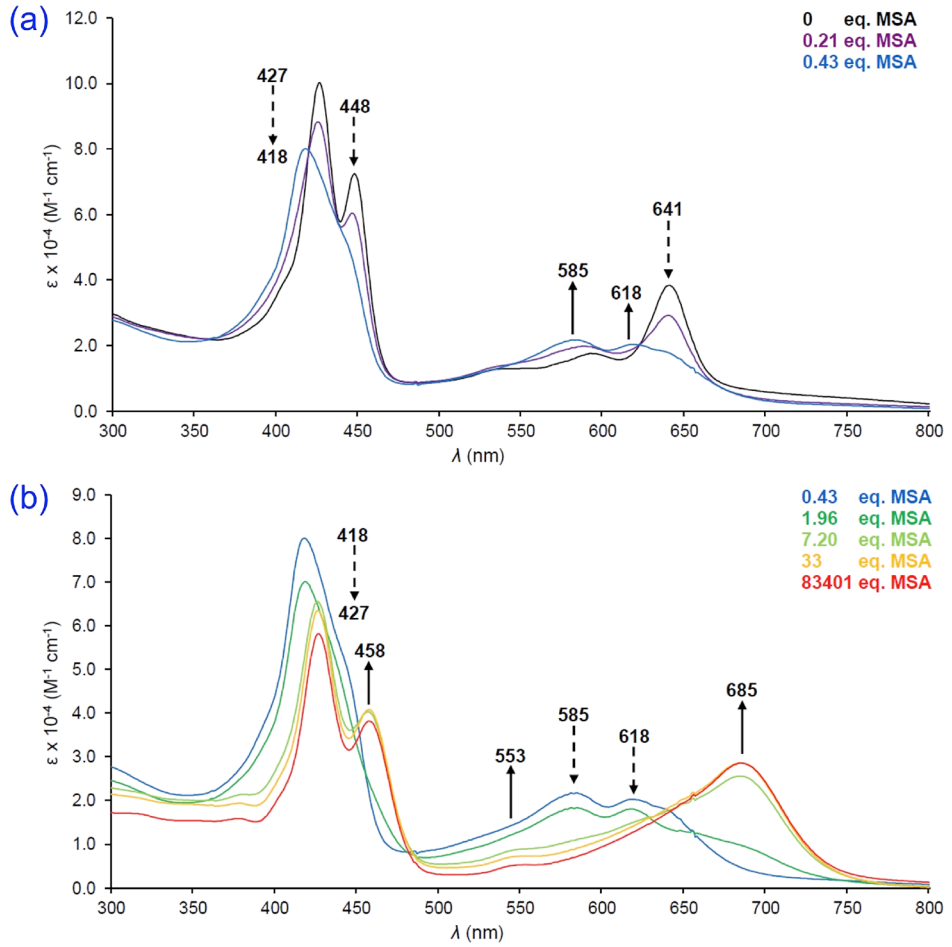

Figure 4. Spectral changes for H_3[TPC] in DMSO as a function of added equivalents of MSA. The two panels approximately correspond to the following transformations: (a) $CorH_2^-$ → $CorH_3$ and (b) $CorH_3$ → $CorH_4^+$.

solution was stirred with a small stir bar and allowed to settle for 3 min before the spectrum was recorded. All titrations were repeated several times on different batches of freshly made corrole.

AUTHOR INFORMATION

Corresponding Author

Abhik Ghosh − *Department of Chemistry, UiT − The Arctic University of Norway, Tromsø N-9037, Norway;* orcid.org/0000-0003-1161-6364; Email: abhik.ghosh@uit.no

Author

Ivar K. Thomassen − *Department of Chemistry, UiT − The Arctic University of Norway, Tromsø N-9037, Norway;* orcid.org/0000-0001-7592-6260

Complete contact information is available at: https://pubs.acs.org/10.1021/acsomega.0c01068

Notes

The authors declare no competing financial interest.

ACKNOWLEDGMENTS

This work was supported by Research Council of Norway (grant no. 262229 to AG) and the Arctic Center for Sustainable Energy at UiT − The Arctic University of Norway. We also thank Prof. Carl Wamser for stimulating discussions.

REFERENCES

(1) Gouterman, M.; Wagnière, G. H.; Snyder, L. C. Spectra of Porphyrins: Part II. Four-Orbital Model. *J. Mol. Spectrosc.* **1963**, *11*, 108−127.

(2) Gouterman, M. Optical Spectra and Electronic Structure of Porphyrins and Related Rings. In *The Porphyrins*; Dolphin, D., Ed.; Academic Press: New York, 1978; Vol. *III, Part A*, pp 1−165.

(3) Sakurai, H.; Yoshimura, T. Models for coordination site of cytochrome P-450, characterization of hemin-thiolato complexes with S, O, and N donor ligands by electronic absorption. *J. Inorg. Biochem.* **1985**, *24*, 75−96.

(4) Sono, M.; Dawson, J. H.; Hager, L. P. The generation of a hyperporphyrin spectrum upon thiol binding to ferric chloroperoxidase. Further evidence of endogenous thiolate ligation to the ferric enzyme. *J. Biol. Chem.* **1984**, *259*, 13209−13216.

(5) Ojadi, E. C. A.; Linschitz, H.; Gouterman, M.; Walter, R. I.; Lindsey, J. S.; Wagner, R. W.; Droupadi, P. R.; Wang, W. Sequential Protonation of *meso*-[*p*-(Dimethylamino)phenyl]porphyrins: Charge-Transfer Excited States Producing Hyperporphyrins. *J. Phys. Chem.* **1993**, *97*, 13192−13197.

(6) Vitasovic, M.; Gouterman, M.; Linschitz, H. Calculations on the origin of hyperporphyrin spectra in sequentially protonated *meso*-(dimethylaminophenyl) porphyrins. *J. Porphyrins Phthalocyanines* **2001**, *05*, 191−197.

(7) Wasbotten, I. H.; Conradie, J.; Ghosh, A. Electronic Absorption and Resonance Raman Signatures of Hyperporphyrins and Nonplanar Porphyrins. *J. Phys. Chem. B* **2003**, *107*, 3613−3623.

(8) Weinkauf, J. R.; Cooper, S. W.; Schweiger, A.; Wamser, C. C. Substituent and Solvent Effects on the Hyperporphyrin Spectra of

https://dx.doi.org/10.1021/acsomega.0c01068
ACS Omega 2020, 5, 9023−9030

Diprotonated Tetraphenylporphyrins. *J. Phys. Chem. A* **2003**, *107*, 3486−3496.
(9) Rudine, A. B.; DelFatti, B. D.; Wamser, C. C. Spectroscopy of Protonated Tetraphenylporphyrins with Amino/Carbomethoxy Substituents: Hyperporphyrin Effects and Evidence for a Monoprotonated Porphyrin. *J. Org. Chem.* **2013**, *78*, 6040−6049.
(10) Wang, C.; Wamser, C. C. Hyperporphyrin Effects in the Spectroscopy of Protonated Porphyrins with 4-Aminophenyl and 4-Pyridyl *Meso* Substituents. *J. Phys. Chem. A* **2014**, *118*, 3605−3615.
(11) Wang, C.; Wamser, C. C. NMR Study of Hyperporphyrin Effects in the Protonations of Porphyrins with 4-Aminophenyl and 4-Pyridyl Meso Substituents. *J. Org. Chem.* **2015**, *80*, 7351−7359.
(12) Milgrom, L. R.; Jones, C. C.; Harriman, A. Facile aerial oxidation of a porphyrin. Part 3. Some metal complexes of *meso*-tetrakis-(3,5-di-t-butyl-4-hydroxyphenyl)porphyrin. *J. Chem. Soc., Perkin Trans. 2* **1988**, 71−79.
(13) Manna, B. K.; Bera, S. C.; Rohatgi-Mukherjee, K. K. Effect of solvent and pH on the spectral characteristics of meso-tetrakis(p-hydroxyphenyl) porphyrin in dimethylformamide and dimethylformamide + water mixed solvents. *Spectrochim. Acta A* **1995**, *51*, 1051−1060.
(14) Guo, H.; Jiang, J.; Shi, Y.; Wang, Y.; Wang, Y.; Dong, S. Sequential Deprotonation of *meso*-(*p*-Hydroxyphenyl)porphyrins in DMF: From Hyperporphyrins to Sodium Porphyrin Complexes. *J. Phys. Chem. B* **2006**, *110*, 587−594.
(15) Ghosh, A.; Wondimagegn, T.; Parusel, A. B. J. Electronic Structure of Gallium, Copper, and Nickel Complexes of Corrole. High-Valent Transition Metal Centers Versus Noninnocent Ligands. *J. Am. Chem. Soc.* **2000**, *122*, 5100−5104.
(16) Alemayehu, A.; Conradie, J.; Ghosh, A. A First TDDFT Study of Metallocorrole Electronic Spectra: Copper *meso*-Triarylcorroles Exhibit *Hyper* Spectra. *Eur. J. Inorg. Chem.* **2011**, *2011*, 1857−1864.
(17) Ghosh, A. Electronic Structure of Corrole Derivatives: Insights from Molecular Structures, Spectroscopy, Electrochemistry, and Quantum Chemical Calculations. *Chem. Rev.* **2017**, *117*, 3798−3881.
(18) Ganguly, S.; Ghosh, A. Seven Clues to Ligand Noninnocence: The Metallocorrole Paradigm. *Acc. Chem. Res.* **2019**, *52*, 2003−2014.
(19) Ganguly, S.; McCormick, L. J.; Conradie, J.; Gagnon, K. J.; Sarangi, R.; Ghosh, A. Electronic Structure of Manganese Corroles Revisited: X-ray Structures, Optical and X-ray Absorption Spectroscopies, and Electrochemistry as Probes of Ligand Noninnocence. *Inorg. Chem.* **2018**, *57*, 9656−9669.
(20) Steene, E.; Wondimagegn, T.; Ghosh, A. Electrochemical and Electronic Absorption Spectroscopic Studies of Substituent Effects in Iron(IV) and Manganese(IV) Corroles. Do the Compounds Feature High-Valent Metal Centers or Noninnocent Corrole Ligands? Implications for Peroxidase Compound I and II Intermediates. *J. Phys. Chem. B* **2001**, *105*, 11406−11413; *J. Phys. Chem. B* **2002**, *106*, 5312−5312.
(21) Steene, E.; Dey, A.; Ghosh, A. β-Octafluorocorroles. *J. Am. Chem. Soc.* **2003**, *125*, 16300−16309.
(22) Walker, F. A.; Licoccia, S.; Paolesse, R. Iron Corrolates: Unambiguous Chloroiron(III) $(Corrolate)^{2-\cdot}$ π-Cation Radicals. *J. Inorg. Biochem.* **2006**, *100*, 810−837.
(23) Ganguly, S.; Giles, L. J.; Thomas, K. E.; Sarangi, R.; Ghosh, A. Ligand Noninnocence in Iron Corroles: Insights from Optical and X-ray Absorption Spectroscopies and Electrochemical Redox Potentials. *Chem. - Eur. J.* **2017**, *23*, 15098−15106.
(24) Vazquez-Lima, H.; Norheim, H.-K.; Einrem, R. F.; Ghosh, A. Cryptic Noninnocence: FeNO Corroles in a New Light. *Dalton Trans.* **2015**, *44*, 10146−10151.
(25) Norheim, H.-K.; Capar, J.; Einrem, R. F.; Gagnon, K. J.; Beavers, C. M.; Vazquez-Lima, H.; Ghosh, A. Ligand Noninnocence in FeNO Corroles: Insights from β-Octabromocorrole Complexes. *Dalton Trans.* **2016**, *45*, 681−689.
(26) Ganguly, S.; Renz, D.; Giles, L. J.; Gagnon, K. J.; McCormick, L. J.; Conradie, J.; Sarangi, R.; Ghosh, A. Cobalt- and Rhodium-Corrole-Triphenylphosphine Complexes Revisited: the Question of a Non-innocent Corrole. *Inorg. Chem.* **2017**, *56*, 14788−14800.
(27) Ganguly, S.; Conradie, J.; Bendix, J.; Gagnon, K. J.; McCormick, L. J.; Ghosh, A. Electronic Structure of Cobalt−Corrole−Pyridine Complexes: Noninnocent Five-Coordinate Co(II) Corrole−Radical States. *J. Phys. Chem. A* **2017**, *121*, 9589−9598.
(28) Jiang, X.; Naitana, M. L.; Desbois, N.; Quesneau, V.; Brandès, S.; Rousselin, Y.; Shan, W.; Osterloh, W. R.; Blondeau-Patissier, V.; Gros, C. P.; Kadish, K. M. Electrochemistry of Bis(pyridine)cobalt (Nitrophenyl)corroles in Nonaqueous Media. *Inorg. Chem.* **2018**, *57*, 1226−1241.
(29) Wasbotten, I. H.; Wondimagegn, T.; Ghosh, A. Electronic Absorption, Resonance Raman, and Electrochemical Studies of Planar and Saddled Copper(III) *meso*-Triarylcorroles. Highly Substituent-Sensitive Soret Bands as a Distinctive Feature of High-Valent Transition Metal Corroles. *J. Am. Chem. Soc.* **2002**, *124*, 8104−8116.
(30) Thomas, K. E.; Wasbotten, I. H.; Ghosh, A. Copper β-Octakis(Trifluoromethyl)Corroles: New Paradigms for Ligand Substituent Effects in Transition Metal Complexes. *Inorg. Chem.* **2008**, *47*, 10469−10478.
(31) Alemayehu, A. B.; Hansen, L. K.; Ghosh, A. Nonplanar, Noninnocent, and Chiral: A Strongly Saddled Metallocorrole. *Inorg. Chem.* **2010**, *49*, 7608−7610.
(32) Berg, S.; Thomas, K. E.; Beavers, C. M.; Ghosh, A. Undecaphenylcorroles. *Inorg. Chem.* **2012**, *51*, 9911−9916.
(33) Thomas, K. E.; McCormick, L. J.; Carrié, D.; Vazquez-Lima, H.; Simonneaux, G.; Ghosh, A. Halterman Corroles and Their Use as a Probe of the Conformational Dynamics of the Inherently Chiral Copper Corrole Chromophore. *Inorg. Chem.* **2018**, *57*, 4270−4276.
(34) Lim, H.; Thomas, K. E.; Hedman, B.; Hodgson, K. O.; Ghosh, A.; Solomon, E. I. X-ray Absorption Spectroscopy as a Probe of Ligand Noninnocence in Metallocorroles: The Case of Copper Corroles. *Inorg. Chem.* **2019**, *58*, 6722−6730.
(35) Einrem, R. F.; Gagnon, K. J.; Alemayehu, A. B.; Ghosh, A. Metal-Ligand Misfits: Facile Access to Rhenium-Oxo Corroles by Oxidative Metalation. *Chem. - Eur. J.* **2016**, *22*, 517−520.
(36) Alemayehu, A. B.; Gagnon, K. J.; Terner, J.; Ghosh, A. Oxidative Metalation as a Route to Size-Mismatched Macrocyclic Complexes: Osmium Corroles. *Angew. Chem., Int. Ed.* **2014**, *53*, 14411−14414.
(37) Alemayehu, A. B.; Vazquez-Lima, H.; Beavers, C. M.; Gagnon, K. J.; Bendix, J.; Ghosh, A. Platinum Corroles. *Chem. Comm.* **2014**, *50*, 11093−11096.
(38) Alemayehu, A. B.; McCormick, L. J.; Gagnon, K. J.; Borisov, S. M.; Ghosh, A. Stable Platinum(IV) Corroles: Synthesis, Molecular Structure, and Room-Temperature Near-IR Phosphorescence. *ACS Omega* **2018**, *3*, 9360−9368.
(39) Alemayehu, A. B.; Ghosh, A. Gold Corroles. *J. Porphyrins Phthalocyanines* **2011**, *15*, 106−110.
(40) Thomas, K. E.; Alemayehu, A. B.; Conradie, J.; Beavers, C.; Ghosh, A. Synthesis and Molecular Structure of Gold Triarylcorroles. *Inorg. Chem.* **2011**, *50*, 12844−12851.
(41) Thomas, K. E.; Vazquez-Lima, H.; Fang, Y.; Song, Y.; Gagnon, K. J.; Beavers, C. M.; Kadish, K. M.; Ghosh, A. Ligand Noninnocence in Coinage Metal Corroles: A Silver Knife-Edge. *Chem. - Eur. J.* **2015**, *21*, 16839−16847.
(42) Ou, Z.; Shen, J.; Shao, J.; E, W.; Gałęzowski, M.; Gryko, D. T.; Kadish, K. M. Protonated Free-Base Corroles: Acidity, Electrochemistry, and Spectroelectrochemistry of $[(Cor)H_4]^+$, $[(Cor)H_5]^{2+}$, and $[(Cor)H_6]^{3+}$. *Inorg. Chem.* **2007**, *46*, 2775−2786.
(43) Song, Y.; Fang, Y.; Ou, Z.; Capar, J.; Wang, C.; Conradie, J.; Thomas, K. E.; Wamser, C. C.; Ghosh, A.; Kadish, K. M. Influence of β-octabromination on free-base triarylcorroles: Electrochemistry and protonation-deprotonation reactions in nonaqueous media. *J. Porphyrins Phthalocyanines* **2017**, *21*, 633−645.
(44) Collman, J. P.; Decréau, R. A. 5,10,15-Tris(*o*-aminophenyl) Corrole (TAPC) as a Versatile Synthon for the Preparation of Corrole-Based Hemoprotein Analogs. *Org. Lett.* **2005**, *7*, 975−978.
(45) Zhu, W.-H. Synthesis and characterization of two substituted corroles. *Guangpu Shiyanshi* **2013**, *30*, 1562−1566.
(46) Friedman, A.; Landau, L.; Gonen, S.; Gross, Z.; Elbaz, L. *ACS Catal.* **2018**, *8*, 5024−5031.

https://dx.doi.org/10.1021/acsomega.0c01068
ACS Omega 2020, 5, 9023−9030

(47) Mahammed, A.; Weaver, J. J.; Gray, H. B.; Abdelas, M.; Gross, Z. How Acidic Are Corroles and Why? *Tetrahedron Lett.* **2003**, *44*, 2077−2079.
(48) Stone, A.; Fleischer, E. B. The molecular and crystal structure of porphyrin diacids. *J. Am. Chem. Soc.* **1968**, *90*, 2735−2748.
(49) Cheng, B.; Munro, O. Q.; Marques, H. M.; Scheidt, W. R. An Analysis of Porphyrin Molecular FlexibilityUse of Porphyrin Diacids. *J. Am. Chem. Soc.* **1997**, *119*, 10732−10742.
(50) Juillard, S.; Ferrand, Y.; Simonneaux, G.; Toupet, L. Molecular structure of simple mono- and diphenyl meso-substituted porphyrin diacids: influence of protonation and substitution on the distorsion. *Tetrahedron* **2005**, *61*, 3489−3495.
(51) Eriksen, J. J.; Sauer, S. P. A.; Mikkelsen, K. V.; Christiansen, O.; Jensen, H. J. A.; Kongsted, J. Failures of TDDFT in describing the lowest intramolecular charge-transfer excitation in para-nitroaniline. *Mol. Phys.* **2013**, *111*, 1235−1248.
(52) Maitra, N. Charge Transfer in Time-Dependent Density Functional Theory. *J. Phys.: Condens. Matter* **2017**, *29*, 423001.
(53) Kümmel, S. Charge-Transfer Excitations: A Challenge for Time-Dependent Density Functional Theory That Has Been Met. *Adv. Energy Mater.* **2017**, *7*, 1700440.
(54) Bruhn, T.; Brückner, C. The origin of the absorption spectra of porphyrin *N*- and dithiaporphyrin *S*-oxides in their neutral and protonated states. *Phys. Chem. Chem. Phys.* **2015**, *17*, 3560.

https://dx.doi.org/10.1021/acsomega.0c01068
ACS Omega 2020, 5, 9023−9030